

Nonlinear features of the superconductor–ferromagnet–superconductor φ_0 Josephson junction in ferromagnetic resonance region

Aliasghar Janalizadeh¹, Ilhom R. Rahmonov^{2,3,4}, Sara A.

Abdelmoneim⁵, Yury M. Shukrinov^{2,3,4}, and Mohammad R. Kolahchi¹

¹ *Department of Physics, Institute for Advanced Studies in Basic Sciences (IASBS), P.O. Box 45137-66731, Zanjan, Iran*

² *BLTP, JINR, Dubna, Moscow Region, 141980, Russia*

³ *Dubna State University, Dubna, 141980, Russia*

⁴ *Moscow Institute of Physics and Technology, Dolgoprudny, 141700, Moscow Region, Russia*

⁵ *Physics department, Menofiya University, Faculty of Science, 32511, Shebin Elkom, Egypt*

(Dated: October 4, 2022)

We demonstrate the manifestations of the nonlinear features in magnetic dynamics and IV-characteristics of the φ_0 Josephson junction in the ferromagnetic resonance region. We show that at small values of system parameters, namely, damping, spin-orbit interaction, and Josephson to magnetic energy ratio, the magnetic dynamics is reduced to the dynamics of the scalar Duffing oscillator, driven by the Josephson oscillations. The role of increasing superconducting current in the resonance region is clarified. Shifting of the ferromagnetic resonant frequency and the reversal of its damping dependence due to nonlinearity are demonstrated by the full Landau-Lifshitz-Gilbert-Josephson system of equations, and in its different approximations. Finally, we demonstrate the negative differential resistance in the IV-characteristics, and its correlation with the foldover effect.

I. INTRODUCTION

The coupling of superconducting phase difference with magnetic moment of ferromagnet in the φ_0 junction leads to a number of unique features important for superconducting spintronics, and modern information technology [1–5]. It allows to control the magnetization precession by superconducting current and affects the current–voltage (IV) characteristics by magnetic dynamics in the ferromagnet, in particular, to create a DC component in the superconducting current [6–8]. A remarkable manifestation of such coupling is the possibility to stimulate a magnetization reversal in the ferromagnetic layer by applying current pulse through the φ_0 -junction [3, 9–13].

There are two features of our Josephson junction that come into play in our study. One is the broken inversion symmetry in the weak link of the Josephson junction, when the link is magnetic, which introduces an extra phase in the current–phase relation, preventing it from being antisymmetric. Such Josephson junctions are named φ_0 junctions [1], and examples exist such as MnSi and FeGe. Second is the nonlinear property of the system that makes for an anomalous resonance behavior [14].

We couple such a Josephson junction to the model that describes the magnetodynamics in thin films or heterostructure, to form the Landau-Lifshitz-Gilbert-Josephson model (LLGJ)[14–16]. It is shown that for a particular set of parameters, the coupled equations reduce to the dynamics of a Duffing oscillator [14]. The cubic nonlinearity in this oscillator has applications in describing several effects in other models too [17]. One being the resonance effects in the antiferromagnetic bimeron in response to an alternating current, which has applications in the detection of weak signals [15, 18, 19].

The Gilbert damping term is added phenomenologically to the Landau–Lifshitz model, to reproduce the damping of the precessing magnetic moment. Gilbert

damping is important in modeling other resonance features too, as its temperature dependence affects them [20, 21], and in return in the superconducting correlations that affect it [22]. The magnetization precession in the ultra thin $Co_{20}Fe_{60}B_{20}$ layer stimulated by microwave voltage under a large angle, needs modeling by Duffing oscillator too. This gets help from the so called foldover features, again due to nonlinearity [16, 23, 24].

The consequences of the nonlinear nature of the coupled set of LLGJ system of equations in the weak coupling regime was demonstrated recently in Ref. [14]. We showed in this regime, where the Josephson energy is small compared to the magnetic energy, the φ_0 Josephson junction is equivalently described by a scalar nonlinear Duffing equation. An anomalous dependence of the ferromagnetic resonant frequency (FMR) with the increase of the Gilbert damping was found. We showed that the damped precession of the magnetic moment is dynamically driven by the Josephson supercurrent, and the resonance behavior is given by the Duffing spring. The obtained results were based on the numerical simulations. The role of dc superconducting current, and the state with negative differential resistance (NDR) in IV-characteristic were not clarified. Also, the effects of the Josephson to magnetic energy ratio and the spin-orbit coupling (SOC) were not investigated at that time.

In the present paper, we study the nonlinear aspects of the magnetic dynamics and IV-characteristics of the φ_0 Josephson junction in the ferromagnetic resonance region. We compare description of the anomalous damping dependence (ADD) exhibited by full LLGJ system of equations with approximated equations and demonstrate the Duffing oscillator features in the small parameter regime. Effects of the Josephson to magnetic energy ratio, and the spin-orbit coupling on the ADD, referred to earlier as the α -effect [14] are demonstrated. By deriving the formula which couples the dc superconduct-

ing current and maximal amplitude of magnetization we discuss the correlation of superconducting current and the negative differential resistance in the resonance region. Finally, we discuss the experimentally important features by emphasizing the details of the magnetization dynamics and the IV-characteristics of the φ_0 junction.

We have shown that in the limit of small system parameters; that is, the Josephson to magnetic energy ratio G , the damping α , and the spin-orbit coupling r , the dynamics is given by the Duffing spring [14]. We focus on the shift in resonance and the effects of nonlinear interactions. We give semi-analytic models to explain our results in various limits.

The paper is organized as follows. In Section II we outline the theoretical model and discuss the methods of calculations. The ferromagnetic resonance and effects of system parameters on the anomalous damping dependence are considered in Subsection A of Section III. In Subsection B we present analytical description of the dynamics and IV-characteristics of the φ_0 junction at small system parameters. Manifestation of the negative differential resistance in IV-characteristics through the foldover effect is discussed. We compare the description of the anomalous damping dependence by full LLGJ system of equation with approximated equation, and show how the Duffing oscillator captures the nonlinearities in the small parameter regime in Subsection C. We present results on the critical damping and derive the formula which couples the dc superconducting current and maximal amplitude of magnetization in the ferromagnetic layer. Finally, in Section IV we concludes the paper.

II. MODELS AND METHOD

The following section is closely related to our work in [13]. The φ_0 junction [6, 12, 25] that we study is shown in Fig.1. The current-phase relation in φ_0 junction has the form $I_s = I_c \sin(\varphi - \varphi_0)$, where $\varphi_0 = rM_y/M_0$, M_y denotes the component of magnetic moment in \hat{y} direction, M_0 is the modulus of the magnetization. The physics of φ_0 Josephson junction is determined by system of equations which consists of Landau-Lifshits-Gilbert (LLG), resistively capacitively shunted junction (RCSJ) model expression with current-phase relation (I_s) described above, and Josephson relation between phase difference and voltage.

The dynamics of the magnetic moment \mathbf{M} is described by the LLG equation [26]

$$\frac{d\mathbf{M}}{dt} = -\gamma \mathbf{M} \times \mathbf{H}_{eff} + \frac{\alpha}{M_0} \left(\mathbf{M} \times \frac{d\mathbf{M}}{dt} \right), \quad (1)$$

where \mathbf{M} is the magnetization vector, γ is the gyromagnetic relation, \mathbf{H}_{eff} is the effective magnetic field, α is Gilbert damping parameter, $M_0 = |\mathbf{M}|$.

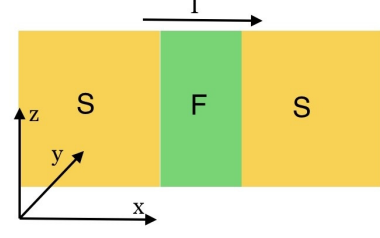


Figure 1. Schematic view of SFS φ_0 Josephson junction. The external current applied along x direction, ferromagnetic easy axis is along z direction.

In order to find the expression for the effective magnetic field we have used the model developed in Ref.[6], where it is assumed that the gradient of the spin-orbit potential is along the easy axis of magnetization taken to be along \hat{z} . In this case the total energy of the system can be written as

$$E_{tot} = -\frac{\Phi_0}{2\pi} \varphi I + E_s(\varphi, \varphi_0) + E_M(\varphi_0), \quad (2)$$

where φ is the phase difference between the superconductors across the junction, I is the external current, $E_s(\varphi, \varphi_0) = E_J [1 - \cos(\varphi - \varphi_0)]$, and $E_J = \Phi_0 I_c / 2\pi$ is the Josephson energy. Here Φ_0 is the flux quantum, I_c is the critical current, $r = lv_{so}/v_F$, $l = 4\hbar L/\hbar v_F$, L is the length of F layer, h is the exchange field of the F layer, $E_M = -K\mathcal{V}M_z^2/(2M_0^2)$, the parameter v_{so}/v_F characterizes a relative strength of spin-orbit interaction, K is the anisotropic constant, and \mathcal{V} is the volume of the ferromagnetic (F) layer.

The effective field for LLG equation is determined by

$$\begin{aligned} \mathbf{H}_{eff} &= -\frac{1}{\mathcal{V}} \frac{\partial E_{tot}}{\partial \mathbf{M}} \\ &= \frac{\Omega_F}{\gamma} \left[Gr \sin\left(\varphi - r \frac{M_y}{M_0}\right) \hat{y} + \frac{M_z}{M_0} \hat{z} \right] \end{aligned} \quad (3)$$

where $\Omega_F = \gamma K/M_0$ is frequency of ferromagnetic resonance and $G = E_J/(K\mathcal{V})$ determines the ratio of Josephson energy to magnetic one.

In order to describe the full dynamics φ_0 junction the LLG equations should be supplemented by the equation for phase difference φ , i.e. equation of RCSJ model for bias current and Josephson relation for voltage. According to the extended RCSJ model, which takes into account derivative of φ_0 phase shift, the current flowing through the system in underdamped case is determined by

$$\begin{aligned} I &= \frac{\hbar C}{2e} \frac{d^2 \varphi}{dt^2} + \frac{\hbar}{2eR} \left[\frac{d\varphi}{dt} - \frac{r}{M_0} \frac{dM_y}{dt} \right] \\ &\quad + I_c \sin\left(\varphi - \frac{r}{M_0} M_y\right). \end{aligned} \quad (4)$$

where I is the bias current, C and R are the capacitance and resistance of Josephson junction respectively. The

Josephson relation for voltage is given by :

$$\frac{\hbar}{2e} \frac{d\varphi}{dt} = V. \quad (5)$$

We note that in the framework of RCSJ-model the displacement current is proportional to the first derivative of voltage (or second derivative of phase difference). From the other hand, the magnetization dynamics plays role of the external force and first order derivative of φ_0 is a source of external current for JJ. This was demonstrated in Ref.[25, 27] where the authors included the first derivative of φ_0 as the source of the electromotive force. Voltage is determined by the phase difference, and does not depend on φ_0 . From this point of view, in the framework of RCSJ model the external current source cannot modify the expression for displacement current. That's why we do not include the second derivative of φ_0 in our model.

Using (1), (3), (4) and (5) we can write the system of equations, in normalised variables, which describes the dynamics of φ_0 junction

$$\begin{aligned} \dot{m}_x &= \frac{\omega_F}{1+\alpha^2} \{-m_y m_z + Gr m_z \sin(\varphi - r m_y) \\ &\quad - \alpha [m_x m_z^2 + Gr m_x m_y \sin(\varphi - r m_y)]\}, \\ \dot{m}_y &= \frac{\omega_F}{1+\alpha^2} \{m_x m_z \\ &\quad - \alpha [m_y m_z^2 - Gr(m_z^2 + m_x^2) \sin(\varphi - r m_y)]\}, \\ \dot{m}_z &= \frac{\omega_F}{1+\alpha^2} \{-Gr m_x \sin(\varphi - r m_y) \\ &\quad - \alpha [Gr m_y m_z \sin(\varphi - r m_y) - m_z(m_x^2 + m_y^2)]\}, \\ \dot{V} &= \frac{1}{\beta_c} [I - V + r \dot{m}_y - \sin(\varphi - r m_y)], \\ \dot{\varphi} &= V \end{aligned} \quad (6)$$

where $m_{x,y,z} = M_{x,y,z}/M_0$ and satisfy the constraint $\sum_{i=x,y,z} m_i^2(t) = 1$, $\beta_c = 2eI_c C R^2 / \hbar$ is McCumber parameter. In order to use the same time scale in the LLG and RCSJ equations in this system of equations we have normalized time to the ω_c^{-1} , where $\omega_c = \frac{2eI_c R}{\hbar}$, and $\omega_F = \Omega_F / \omega_c$ is the normalized frequency of ferromagnetic resonance $\Omega_F = \gamma K / M_0$. Bias current is normalized to the critical current I_c and voltage V – to the $V_c = I_c R$. The system of equations (6), is solved numerically using the fourth-order Runge-Kutta method (see Ref.[14]).

III. RESULTS AND DISCUSSION

A. Effect of system parameters on the anomalous damping dependence

ADD of the FMR frequency with increasing α was discussed in Ref. [14]. It was found that the resonance curves demonstrate features of Duffing oscillator, reflecting the nonlinear nature of Landau-Lifshitz-Gilbert-

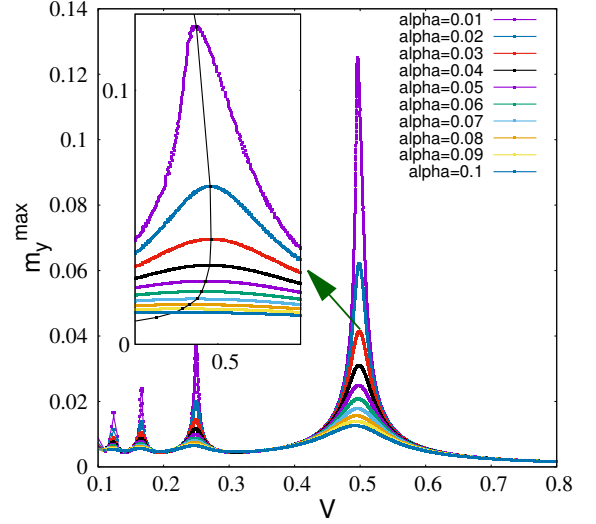


Figure 2. Maximal amplitude of magnetization m_y -component at each values of bias current and voltage along IV-characteristics of the φ_0 junction in the ferromagnetic resonance region for various α . Inset enlarges the main maximum. Parameters: $\beta_c = 25, G=0.05, r=0.05, \omega_F = 0.5$.

Josephson (LLGJ) system of equations. There is a critical damping value at which anomalous dependence comes into play. This critical value depends on the system parameters. Here we present the details of such transformation from usual to anomalous dependence with variation in spin-orbit coupling and ratio of Josephson to magnetic energy.

To investigate the effect of damping, we calculate the maximal amplitude of magnetization component m_y taken at each value of the bias current based on the LLGJ system of equations (6). In Fig.2 we show the voltage dependence of maximal amplitude m_y^{max} in the ferromagnetic resonance region at different damping parameter and small values of Josephson to magnetic energy ratio $G=0.05$ and spin-orbit coupling $r = 0.05$. We found that the ferromagnetic resonance curves demonstrate the different forms. An increase in damping shows a nonuniform change in the resonant frequency: it is approaching the ω_F instead of moving away with increase in α . We stress that this happens at small G and r . We consider that such behavior can be explained by the nonlinear nature of the LLGJ system of equations. There is a manifestation of subharmonics of the FMR in Fig.2 at $\omega = 1/2, 1/3, 1/4$.

We usually expect the resonance peak to move away from resonance as the α increases. Figure 2 shows that this normal effect is accompanied with an anomalous behaviour as can be seen in the inset to this figure, where the resonance peak approaches ω_F as α increases [14].

The manifestation of FMR in IV-characteristics of the φ_0 junction at three values of damping parameter is demonstrated in Fig. 3. The strong deviation of the IV-curve is observing at $\alpha = 0.01$, which is characteristic

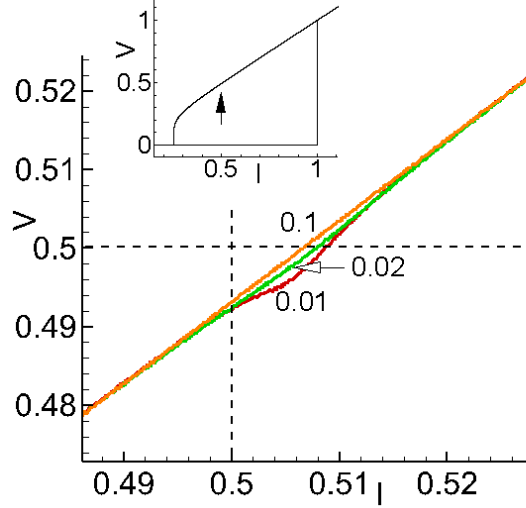


Figure 3. Part of the IV characteristic of the φ_0 junction at $G = 0.05, r = 0.05$ and different values of Gilbert damping. The numbers show α value. Inset shows the total IV-characteristic and arrow indicates the resonance region

value for many magnetic materials. This fact indicates that ADD can be observed experimentally by measuring IV-characteristics in wide interval of the damping parameter.

Interesting features of ADD appear by a variation of spin-orbit coupling. As it was demonstrated in Ref.[28], an increase in SOC leads to the essential change in IV-characteristics and magnetization precession in the ferromagnetic resonance region. The nonlinearity is going stronger and the state with negative differential resistance appears at large SOC.

Figure 4(a) demonstrates results of numerical simulations of m_y^{max} dependence on α at different values of SOC parameter r . It shows two specific features of ADD. First, with an increase in r , the critical value of V_{peak} is decreasing (the curve moves away from ω_F). The second important feature is an increasing of α_{crit} which is demonstrated in this figure by arrows.

Another model parameter which affects the phenomenon discussed in the present paper is the ratio G of Josephson to magnetic energies. Figure 4(b) demonstrates the results of numerical simulations of m_y^{max} dependence on α at different values of G .

Similar to the effect of r , increasing G also causes the value of α_{crit} to increase. By changing the volume of the ferromagnetic layer, the ferromagnetic energy and consequently the value of G can be changed [6]. For small G , i.e. a situation where the magnetic energy is much larger than the Josephson energy, the magnetic layer receives less energy, and its amplitude decreases in the y direction, and also the maximum value of the oscillation frequency is closer to the magnetic frequency, ω_F .

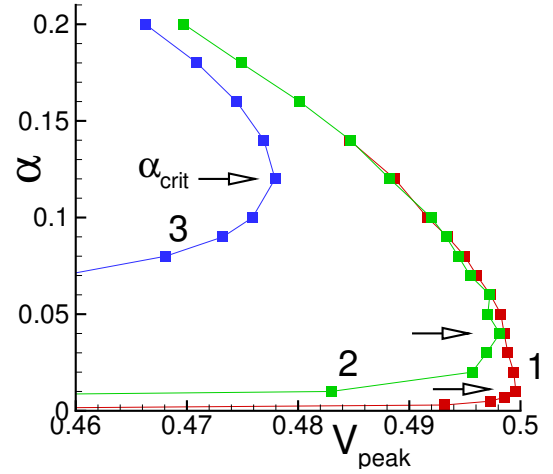
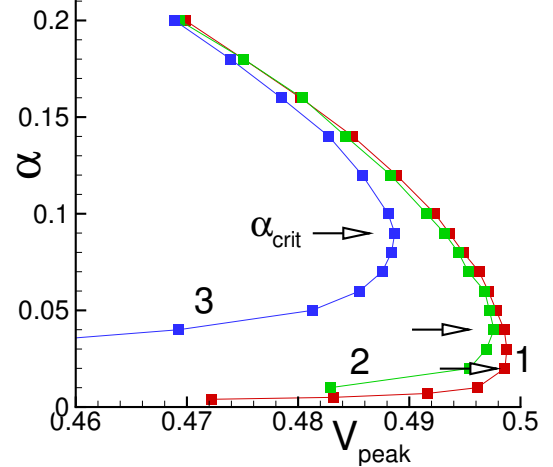


Figure 4. (a) Demonstration of ADD at different values of SOC parameter r at $G = 0.05$. Numbers indicate: 1 - $r = 0.05$; 2 - $r = 0.1$; 3 - $r = 0.5$; Arrows show critical α value, corresponded to the reversal in the α dependence (b) Demonstration of ADD at different values of the Josephson to magnetic energy ratio G at $r = 0.05$. Numbers indicate: 1 - $G = 0.01$; 2 - $G = 0.1$; 3 - $G = 1$.

B. Dynamics and IV-characteristics of the φ_0 junction at small system parameters

As it was discussed in Refs.[6, 29, 30], in case of $G, r, \alpha \ll 1$ and $m_z \approx 1$, first three equations of the system (6) can be simplified. Taking into account $\varphi = \omega_J t$ and neglecting quadratic terms of m_x and m_y , we get

$$\begin{cases} \dot{m}_x = \omega_F [-m_y + Gr \sin(\omega_J t) - \alpha m_x] \\ \dot{m}_y = \omega_F [m_x - \alpha m_y], \end{cases} \quad (7)$$

This system of equations can be written as the second order differential equation with respect to m_y

$$\ddot{m}_y + 2\alpha\omega_F \dot{m}_y + \omega_F^2 m_y = \omega_F^2 Gr \sin \omega_J t. \quad (8)$$

Corresponding solution for m_y has the form

$$m_y(t) = \frac{\omega_+ - \omega_-}{r} \sin(\omega_J t) - \frac{\gamma_+ + \gamma_-}{r} \cos(\omega_J t), \quad (9)$$

where

$$\omega_{\pm} = \frac{Gr^2\omega_F}{2} \frac{\omega_J \pm \omega_F}{\Omega_{\pm}}, \quad (10)$$

and

$$\gamma_{\pm} = \frac{Gr^2\omega_F}{2} \frac{\alpha\omega_J}{\Omega_{\pm}}. \quad (11)$$

with $\Omega_{\pm} = (\omega_J \pm \omega_F)^2 + (\alpha\omega_J)^2$ (see Ref.[6] and corresponded Erratum[31]).

When the Josephson frequency ω_J is approaching the ferromagnetic one ω_F , m_y demonstrates the damped ferromagnetic resonance. Differential resistance in the resonance region is decreasing and it is manifested in the IV-characteristic as a resonance branch [7].

Taking into account $rm_y \ll 1$, we rewrite expression for superconducting current as

$$\begin{aligned} I_s(t) &= \sin(\omega_J t - rm_y(t)) \\ &= \sin(\omega_J t) - rm_y \cos(\omega_J t) \end{aligned} \quad (12)$$

Using solution (9) we can obtain

$$\begin{aligned} I_s(t) &= \sin \omega_J t - \frac{\omega_+ - \omega_-}{2} \sin 2\omega_J t \\ &+ \frac{\gamma_+ + \gamma_-}{2} \cos 2\omega_J t + I_0(\alpha) \end{aligned} \quad (13)$$

where

$$I_0 = \frac{\gamma_+ + \gamma_-}{2}. \quad (14)$$

This superconducting current explains the appearance of the resonance branch in the IV-characteristic. The generated current I_0 can be expressed through the amplitude of m_y and SOI parameter r

$$I_0 = \frac{r}{2} m_y^{max}(\omega_J), \quad (15)$$

with $m_y^{max}(\omega_J)$ being the frequency response of m_y .

At small model parameters $\alpha \ll Gr \ll 1$ of SFS φ_0 Josephson junction, the states with a negative differential resistance appear in the IV-characteristics in the FMR region. Due to the nonlinearity, the resonance peak is asymmetric. Increasing of nonlinearity leads to the bistability (foldover effect). A natural questions appears if the states with a negative differential resistance are the origin of the foldover and ADD. In order to clarify this question, we show in Fig.5 a part of IV-characteristics of φ_0 junction together with IV-characteristic of SIS junction in the ferromagnetic resonance region and numerically calculated superconducting current through this junction. The total IV-characteristics are demonstrated in the inset to this figure.

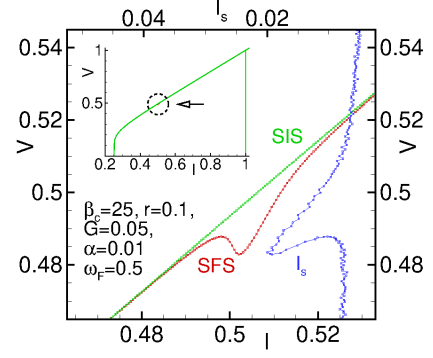


Figure 5. IV-characteristic of φ_0 and SIS junctions and calculated average superconducting current through the φ_0 junction.

We see the correlation of the foldover effect in superconducting current (blue) with the NDR part of IV-curve. The peak in the superconducting current and minimum of IV-curve are at the same voltage value. So, both effects reflect the nonlinear features of the ferromagnetic resonance in φ_0 junction. But in contrast to the foldover and ADD effects, which start manifesting themselves at relatively small deviations from linear case, the nonlinearity in case of the NDR plays a more essential role.

We note that in the resonance region for considered limit of model parameters the m_y amplitude are coupled to the value of superconducting current (see Eq.(15)). We stress the importance of the performed analysis demonstrating the analytical coupling of time independent superconducting current and magnetization, reflecting the Duffing oscillator features of the φ_0 junction.

As it is well known, the states with negative differential resistance appear in IV-characteristics of Josephson structures in different physical situations. In particular, the nonlinear superconducting structures being driven far from equilibrium exhibit NDR states [32]. The NDR states plays an essential role in the applications related to the THz radiation emission [33]. A detailed explanation for different types of negative differential resistance (NDR) in Josephson junction (i.e., N-shaped and S-shaped) is introduced in[34]. The authors emphasize that the nonlinear behavior of the Josephson junction plays a key role in the NDR feature. In our case, the NDR states appear as a result of system's nonlinearity at small values of φ_0 junction parameters, such as SOC, ratio of Josephson to magnetic energy and Gilbert damping. We demonstrate these effects here by by presented results of detailed investigation of the NDR state at different system parameters and discuss possibility of their control near the ferromagnetic resonance.

Figure 6 shows the effect of the spin-orbit coupling on the IV-characteristic at $G = 0.05$ and $\alpha = 0.01$. We see the NDR feature which is getting more pronounced with increase in r . A further increase in r leads to the jump down in voltage and then practically linear growth

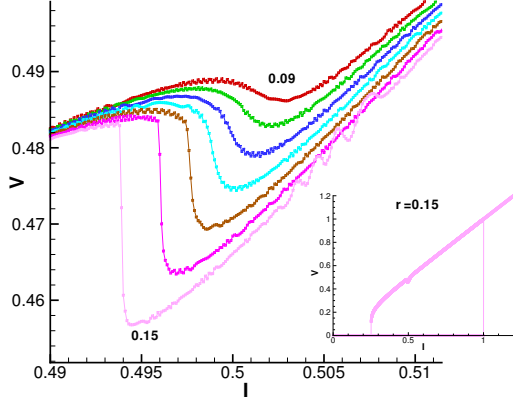


Figure 6. Enlarged parts of the IV-curves in the resonance region at different values of SOC parameter r at $\alpha = 0.01$ and $G = 0.05$. The numbers indicate the increasing of r from 0.09 to 0.15 with an increment 0.01. Inset demonstrates total IV-characteristic at $r = 0.15$

of IV-characteristic.

An interesting question is concerning the effect of Gilbert damping. Results of IV-characteristics simulations in the resonance region at a certain range of the damping parameter α at $G = 0.05$ and $r = 0.13$ are shown in Fig.7(a). In this case, the most pronounced characteristic appears at $\alpha = 0.01$. At chosen set of parameters $G = 0.05$ and $r = 0.13$, the range of α with pronounced NDR features is $0.01 \leq \alpha < 0.014$.

The maximal amplitude m_y^{max} as a function of voltage is shown in Fig.7(b). Based on the results, presented in Fig.7(a) and Fig.7(b), we came to the important conclusion that the foldover effect (bistability) and NDR state have strong correlations and have the same origin related to the nonlinearity at small system parameters.

But anomalous damping dependence does not show a one-to-one correlation with either negative differential resistance or foldover effect. The resonance peak positions of m_y^{max} in bias current I_{peak} , and in voltage V_{peak} as the functions of α are demonstrated in Fig.7(c). According to our results, we can divide α interval into two regions (see Fig.7(c)). Region I introduces the values of α where the NDR feature is present, while in the Region II it disappears. In the Region II the foldover effect (bistability) disappears as well, but ADD is realized.

C. C. Duffing oscillator features of φ_0 junction and critical damping

The system of equations (6) is nonlinear and very complex, so in order to provide analytical study of dynamics of the φ_0 junction we need to derive an approximated equation for some limited values of model parameters. In Ref. [14] was shown that the resonance curves demonstrate features of Duffing oscillator, reflecting the nonlinear nature of Landau-Lifshitz-Gilbert-Josephson (LLGJ)

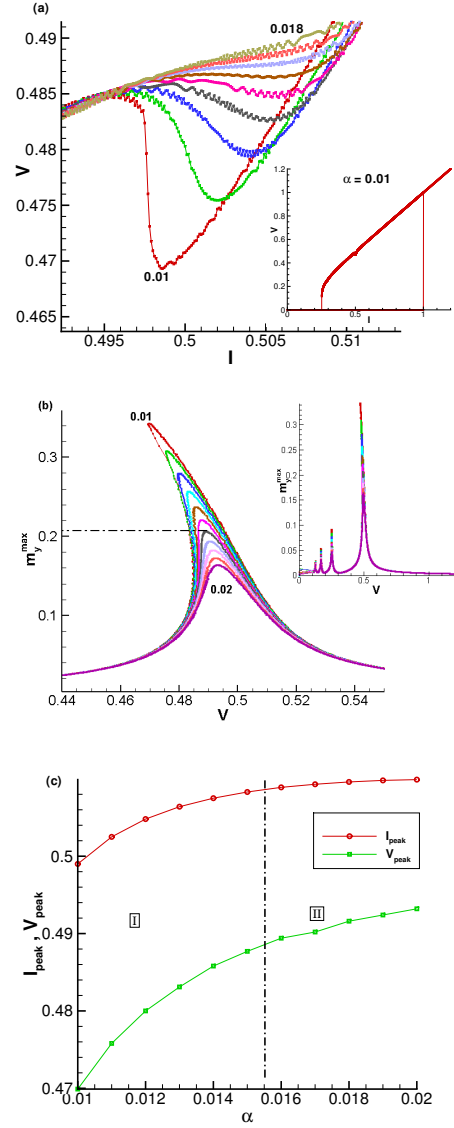


Figure 7. (a) Enlarged parts of the IV-curves at different values of α ; (b) Voltage dependence of m_y^{max} at different α ; (c) α -dependence of the resonance curve maximum in current (I_{peak}) and voltage (V_{peak}). The numbers indicate the value of α from 0.01 to 0.018 in (a) and from 0.01 to 0.02 in (b) by an increment 0.001. Results are obtained at $r = 0.13$, and $G = 0.05$.

system of equations. In this section, we present analytical approach to describe the nonlinear dynamics of φ_0 -junction and compare analytical results followed from approximated Duffing equation with numerical simulations of total system of equations (6). We show that in the limit of $\alpha \ll G, r \ll 1$, we arrive to the Duffing oscillator. We start by first three equations of the (6) for

magnetization components

$$\begin{aligned}\frac{\dot{m}_x}{\omega_F} &= -m_y m_z + Gr m_z \sin(\varphi - r m_y) - \alpha m_x m_z^2 \\ \frac{\dot{m}_y}{\omega_F} &= m_x m_z - \alpha m_y m_z^2 \\ \frac{\dot{m}_z}{\omega_F} &= -Gr m_x \sin(\varphi - r m_y) + \alpha m_z (m_x^2 + m_y^2)\end{aligned}\quad (16)$$

Simplifying this system of equations by the same procedure as it was done in Ref.[14] we can write equation for m_y as

$$\ddot{m}_y + 2\xi\alpha\dot{m}_y + \xi^2(1+\alpha^2)m_y - \xi^2(1+\alpha^2-\alpha^4)m_y^3 = \xi^2\gamma\sin\varphi. \quad (17)$$

Finally, by neglecting the α^2 and α^4 terms which are much smaller than 1, we come to well known Duffing equation,

$$\ddot{m}_y + 2\omega_F\alpha\dot{m}_y + \omega_F^2 m_y - \omega_F^2 m_y^3 = \omega_F^2 Gr \sin\varphi. \quad (18)$$

In the small parameter range, this Duffing equation can describe the dynamics of m_y . We will have the full dynamics, once we consider the coupling with the Josephson equation,

$$\ddot{\varphi} + \frac{1}{\beta_c} [\dot{\varphi} - r\dot{m}_y + \sin(\varphi - r m_y)] = \frac{1}{\beta_c} I. \quad (19)$$

The system of equations, (18) and (19) can replace the LLGJ equations in the limit of $G, r \ll 1$ and $G, r \gg \alpha$.

Taking into account $\varphi = \omega_J t$ we can right analytically obtained frequency response for equation (18)

$$(m_y^{max})^2 = \frac{(Gr)^2}{[\omega^2 - 1 + \frac{3}{4}(m_y^{max})^2]^2 + (2\alpha\omega)^2} \quad (20)$$

where $\omega = \omega_J/\omega_F$. From Eq. (20) we get

$$\begin{aligned}(m_y^{max})^6 + \frac{8}{3}(\omega^2 - 1)(m_y^{max})^4 \\ + \left(\frac{4}{3}\right)^2 \left[(\omega^2 - 1)^2 + (2\alpha\omega)^2 \right] (m_y^{max})^2 \\ - \left(\frac{4}{3}Gr\right)^2 = 0.\end{aligned}\quad (21)$$

This equation allows to determine analytically frequency dependence of the m_y^{max} amplitude. To find it we solve the equation (21) by the Newton method. Results of analytical calculations (blue dots) corresponded to (21) and numerical one (red dotted line) corresponded to the full system of equation (6) are demonstrated in Fig.8.

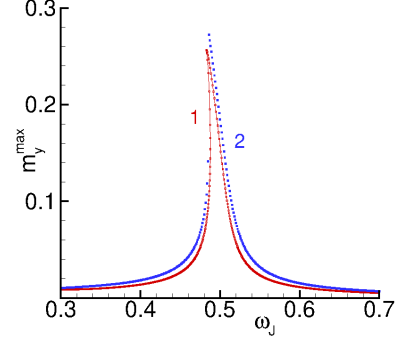


Figure 8. Numerically (curve 1) and analytically (curve 2) calculated amplitude dependence of m_y .

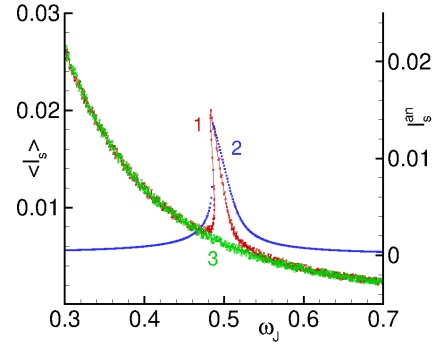


Figure 9. Numerically calculated superconducting current for SFS junction (plot 1) and analytical I_0 (plot 2) and superconducting current for SIS junction (plot 3).

We can see that they are close to each other which proves the correctness of the chosen approximation. Both curves demonstrate an asymmetric resonance peak, which is common for Duffing oscillator. When a role of the cubic term is getting larger, we observe a bistability of the resonance curve, which is usually called a foldover effect. Note that the foldover effect can be also achieved by the damping decreasing; i.e., by the decreasing of dissipative term in (18), we can increase the influence of the cubic term in this equation.

The comparison of analytically and numerically calculated superconducting current as a function of the Josephson frequency is demonstrated in Fig. 9. We note that in our normalization $V = \omega_J$. We can see the manifestation of the asymmetric resonance peak in the frequency dependence of superconducting current. So, the approximated system of equations 7 reflects one of the main feature of Duffing oscillator.

Figure (10) compares anomalous damping dependence of the resonance peak of $m_y^{max}(V)$ calculated numerically according to the full LLGJ system of equations (6) with calculated numerically according to the generalized Duffing model (equations (17, 19)). We see that in the damping parameter interval $[0.001 - 0.2]$ the coincidence

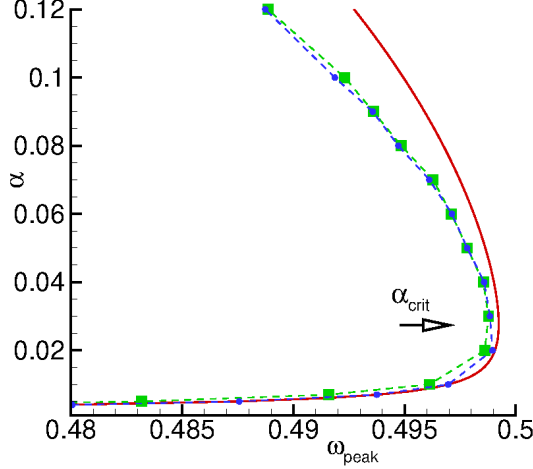


Figure 10. The α -dependence of the resonance maximum of $m_y^{max}(V)$ in the damping parameter interval $[0.001 - 0.12]$. Green squares show results calculated numerically according to the full system of equations (6), blue circles show results calculated numerically according to the generalized Duffing and Josephson equations (17,19). The dashed line connects the symbols to guide eyes. Solid line show analytical α -dependence calculated according to the Eq. (22). All calculation have been done at $\beta_c = 25$, $G=0.05$, $r=0.05$, $\omega_F = 0.5$.

of the dependences is enough good.

Using equation (18) with $\varphi = \omega_J t$, we can find (see Supplementary materials ??) a relation between position of the resonance peak in $m_y^{max}(V)$ dependence and damping

$$\omega_{peak} = \sqrt{\frac{1-3\alpha^2}{2} + \frac{1}{2}\sqrt{(1-\alpha^2)^2 - 12\left(\frac{Gr}{4\alpha}\right)^2}} \quad (22)$$

where $\omega_{peak} = \frac{\omega_{J,peak}}{\omega_F}$ determines the position of the resonance peak.

Equation (22) allows to find the formula for critical damping α_{crit} which is an important parameter determining the reversal point in damping dependence of the resonance peak of $m_y^{max}(V)$.

Taking into account equation (22) we can write equation with respect of $Gr/(4\alpha)$ (See supplementary materials ??).

$$9\left(\frac{Gr}{4\alpha_{crit}}\right)^4 + 3\alpha_{crit}^2(10\alpha_{crit}^2 - 1)\left(\frac{Gr}{4\alpha_{crit}}\right)^2 - 2\alpha_{crit}^4(\alpha_{crit}^2 - 1)^2 = 0 \quad (23)$$

Using approximation $10\alpha_{crit}^2 \ll 1$ and $\alpha_{crit}^2 \ll 1$ it gives (see Supplementary Materials)

$$\alpha_{crit} \approx \frac{1}{2}\sqrt{\frac{3}{2}Gr} \quad (24)$$

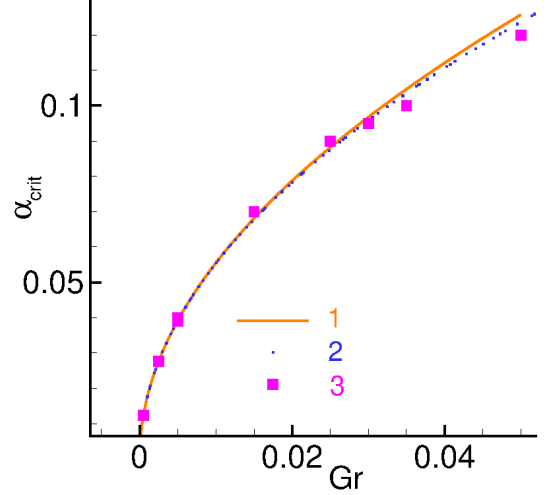


Figure 11. Numerical calculations according to Eq. (6) (squares), analytical according to Eq. (23)(solid line) and approximated analytical according to Eq. (24) (dashed line).

Table 1: A comparison between the numerical and analytical values of $\alpha_{crit.}$ at different values of G and r .

G	r	Gr	$\alpha_{crit.}, numerics$	$\alpha_{crit.}, analytics$
0.01	0.05	0.0005	0.0100	0.0123
0.05	0.05	0.0025	0.0300	0.0276
0.05	0.10	0.0050	0.0400	0.0391
0.05	0.30	0.0150	0.0700	0.0677
0.05	0.50	0.0250	0.0900	0.0874
0.10	0.05	0.0050	0.0391	0.0391
0.60	0.05	0.0300	0.0950	0.0958
0.70	0.05	0.0350	0.1000	0.1035
1.00	0.05	0.0500	0.1200	0.1237

Figure 11 presents comparison of numerical and analytical results α_{crit} versus Gr .

As we see, it shows a good agreement of numerical and analytical results of calculations at small product of Josephson to magnetic energy ratio and spin-orbit interaction.

IV. IV. CONCLUSIONS

The understanding of the nonlinear features of magnetization dynamics in superconductor-ferromagnet-superconductor Josephson junction and their manifestation in the IV-characteristics has implications for superconductor spintronics, and modern information technology. In φ_0 junctions the nonlinear features can affect the control of magnetization precession by superconducting current and external electromagnetic radiation [28].

Here, using numerical and analytic approaches, we have demonstrated that at small system parameters,

namely, the damping, spin-orbit interaction and Josephson to magnetic energy ratio in φ_0 junction, magnetic dynamics is reduced to the dynamics of the scalar Duffing oscillator, driven by the Josephson oscillations. We have clarified the role of increasing superconducting current in the resonance region leading to the foldover effect in the ferromagnet magnetization. We have demonstrated the parameter dependence of the anomalous ferromagnetic resonant shifting with anomalous damping dependence due to nonlinearity of the full LLGJ equation and in its different approximations. We have derived the analytical expression for critical damping value. Also, we demonstrated appearance of negative differential resistance in the IV-characteristics and the correlation with occurrence of the foldover effect in the magnetization of ferromagnet.

We have stressed that the manifestation of negative differential resistance is related to the nonlinear features of the system[34, 35]. It was demonstrated that in the small model parameters case the equation for magnetic subsystem takes form of Duffing equation where nonlinearity manifest itself as the cubic term. We have shown that the appearance of negative differential resistance in the I-V curve is related to the appearance of foldover in

the m_y^{max} -V curve.

We believe that the experimentally measured IV-characteristics of φ_0 junction with manifestations discussed in detail in the present paper, would allow close investigations of its nonlinear features important for superconductor electronics and spintronics.

V. SUPPLEMENTARY

In supplementary material are presented the details of calculations for Eq.22 and Eq.24.

VI. FUNDING

Numerical simulations were funded by Project No. 18-71-10095 of the Russian Science Foundation. The presented results concerning the calculations of DC superconducting current in the section V are supported by the Russian Science Foundation in the framework of project 22-42-04408. A.J. and M.R.K. are grateful to IASBS for financial support.

-
- [1] Buzdin, A. *Physical Review Letters* **2008**, 101 (10), 107005.
 - [2] Linder, J., Robinson, J. W. *Nature Physics* **2015**, 11 (4), 307-315.
 - [3] Bobkova, I., Bobkov, A., Silaev, M. *Physical Review B* **2018**, 98 (1), 014521.
 - [4] Bobkova, I., Bobkov, A., Rahmonov, I., Mazanik, A.; Sengupta, K., Shukrinov, Y. M. *Physical Review B* **2020**, 102 (13), 134505.
 - [5] Szombati, D., Nadj-Perge, S., Car, D., Plissard, S., Bakkers, E., Kouwenhoven, L. *Nature Physics* **2016**, 12 (6), 568–572.
 - [6] Konschelle, F., Buzdin, A. *Physical Review Letters* **2009**, 102 (1), 017001.
 - [7] Shukrinov, Y. M., Rahmonov, I., Sengupta, K. *Physical Review B* **2019**, 99 (22), 224513.
 - [8] Shukrinov, Y. M. *Physics-Uspekhi* **2022**, 65 (4), 317.
 - [9] Linder, J., Yokoyama, T. *Physical Review B* **2011**, 83 (1), 012501.
 - [10] Hoffman, S., Blanter, Y. M., Tserkovnyak, Y. *Physical Review B* **2012**, 86 (5), 054427.
 - [11] Eschrig, M. *Reports on Progress in Physics* **2015**, 78 (10), 104501.
 - [12] Shukrinov, Y. M., Rahmonov, I., Sengupta, K., Buzdin, A. *Applied Physics Letters* **2017**, 110 (18), 182407.
 - [13] Mazanik, A., Rahmonov, I., Botha, A., Shukrinov, Y. M. *Physical Review Applied* **2020**, 14 (1), 014003.
 - [14] Shukrinov, Y. M., Rahmonov, I., Janalizadeh, A., Kollahchi, M. *Physical Review B* **2021**, 104 (22), 224511.
 - [15] Shen, L., Xia, J., Zhang, X., Ezawa, M., Tretiakov, O. A., Liu, X., Zhao, G., Zhou, Y. *Physical review letters* **2020**, 124 (3), 037202.
 - [16] Azovtsev, A. V., Nikitchenko, A. I., Pertsev, N. A. *Physical Review Materials* **2021**, 5 (5), 054601.
 - [17] Zhu, J., Zhang, T., Yang, Y., Huang, R. *Applied Physics Reviews* **2020**, 7 (1), 011312.
 - [18] Wang, G., Chen, D., Lin, J., Chen, X. *IEEE Transactions on industrial electronics* **1999**, 46 (2), 440–444.
 - [19] Almog, R., Zaitsev, S., Shtempluck, O., Buks, E. *Physical Review Letters* **2007**, 98 (7), 078103.
 - [20] Zhao, Y., Song, Q., Yang, S.-H., Su, T., Yuan, W., Parkin, S. S., Shi, J., Han, W. *Scientific reports* **2016**, 6 (1), 1–8.
 - [21] Yao, Y., Song, Q., Takamura, Y., Cascales, J. P., Yuan, W., Ma, Y., Yun, Y., Xie, X., Moodera, J. S., Han, W. *Physical Review B* **2018**, 97 (22), 224414.
 - [22] Silaev, M. *Physical Review B* **2020**, 102 (14), 144521.
 - [23] Nayfeh, A., Mook, D. *Nonlinear Oscillations*. John Wiley & Sons, 1979.
 - [24] Chen, W., De Loubens, G., Beaujour, J.-M., Sun, J., Kent, A. *Applied Physics Letters* **2009**, 95 (17), 172513.
 - [25] Guarcello, C., Bergeret, F. *Physical Review Applied* **2020**, 13 (3), 034012.
 - [26] Landau, L., Lifshitz, E. *Phys. Rev* **1955**, 100, 1243.
 - [27] Rabinovich, D. S., Bobkova, I. V., Bobkov, A. M., Silaev, M. A. *Phys. Rev. Lett.* **2019**, 123, 207001. doi: 10.1103/PhysRevLett.123.207001.
 - [28] Abdelmoneim, S., Shukrinov, Y. M., Kulikov, K., ElSamman, H., Nashaat, M. *Phys. Rev. B* **2022**, 106, 014505.
 - [29] Shukrinov, Y. M., Rahmonov, I. *Physics of Particles and Nuclei* **2020**, 51 (4), 816–822.
 - [30] Shukrinov, Y. M., Rahmonov, I., Botha, A. *Low Temperature Physics* **2020**, 46 (9), 932–938.
 - [31] Konschelle, F., Buzdin, A. *Physical Review Letters* **2019**, 123 (16), 169901.

- [32] Pedersen, N. F., Filatrella, G., Pierro, V., Sørensen, M. P. *Physica C: Superconductivity and its Applications* **2014**, *503*, 178–182.
- [33] Kadowaki, K., Yamaguchi, H., Kawamata, K., Yamamoto, T., Minami, H., Kakeya, I., Welp, U., Ozyuzer, L., Koshelev, A., Kurter, C., Gray, K., Kwok, W.-K. *Physica C: Superconductivity and its applications* **2008**, *468* (7-10), 634–639.
- [34] Filatrella, G., Pierro, V., Pedersen, N. F., Sørensen, M. P. *IEEE Transactions on Applied Superconductivity* **2014**, *24* (6), 1–7.
- [35] Nagel, J., Speer, D., Gaber, T., Sterck, A., Eichhorn, R., Reimann, P., Ilin, K., Siegel, M., Koelle, D., Kleiner, R. *Physical Review Letters* **2008**, *100*, 217001.